Available online at www.sciencedirect.com
SCIENCE DIRECT
Thermochimica Acta 441 (2006) 144–149
thermochimica acta
www.elsevier.com/locate/tca

Temperature-induced denaturation of Aes acetyl-esterase from *Escherichia coli*

Pompea Del Vecchio [a,*], Giuseppe Graziano [b], Guido Barone [a], Luigi Mandrich [c], Mosè Rossi [c], Giuseppe Manco [c]

[a] *Department of Chemistry, University of Naples "Federico II", Via Cintia, 45-80126 Naples, Italy*
[b] *Department of Biological and Environmental Sciences, University of Sannio, Via Port'Arsa, 11-82100 Benevento, Italy*
[c] *Institute of Protein Biochemistry, C.N.R., Via P. Castellino, 111-80131 Naples, Italy*

Received 27 September 2005; received in revised form 5 December 2005; accepted 5 December 2005

Abstract

The thermal stability of the Aes acetyl esterase from *Escherichia coli* has been investigated by means of differential scanning calorimetry and circular dichroism measurements. The calorimetric curves show a denaturation temperature of 68 °C for Aes and 61 °C for the single point mutant V20D-Aes. The same values are obtained from CD denaturation curves of the two proteins recorded in both the far-UV and near-UV regions. Even if the denaturation process is irreversible and characterized by a single calorimetric peak and a single inflection point in both far- and near-UV CD curves, the overall data indicate that the process is more complex than a two-state transition. This is in line with the presence of two structural domains in the 3D model of Aes, according to homology modelling. A comparison of the thermal stability of Aes with those of the homologous thermophilic EST2 and hyperthermophilic AFEST suggests that the optimization of charge–charge interactions should not be so effective in the case of the mesophilic enzyme.

Keywords: α/β Hydrolase fold; Thermal stability; Differential scanning calorimetry; Circular dichroism

1. Introduction

Much efforts have been dedicated in our laboratories to the characterization of two thermophilic esterases, EST2 from *Alicyclobacillus acidocaldarius* and AFEST from *Archeoglobus fulgidus* [1–4], both belonging to the hormone-sensitive lipase, HSL family [5]. In particular we investigated the stability of EST2 and AFEST toward the denaturing action of urea, guanidine hydrochloride, GuHCl, trifluoroethanol, TFE and temperature [6–9]. The discovery that the product of the *ybaC* gene of *Escherichia coli* is an acetyl-esterase, Aes, of the HSL family [10,11], prompted us to characterize the stability of this enzyme as a mesophilic counterpart of EST2 and AFEST.

Aes is a cytoplasmatic protein consisting of 319 residues. Sequence alignments indicate that Aes is homologous to other members of the HSL family. It has a sequence identity of about 30% with brefeldine esterase, BFAE, EST2 and AFEST [12]. Homology modelling, using either the X-ray structure of EST2 [13] or the X-ray structure of BFAE [14], shows that Aes should possess the canonical α/β hydrolase fold with a central β-sheet of eight twisted strands surrounded and partially covered by several α-helical segments. The 3D structure of Aes has not been determined so far, but preliminary X-ray data on Aes crystals have been collected [12,15].

With the aim to perform a comparative analysis with a mesophilic member of the HLS family, in a previous study we investigated the conformational stability of Aes toward the denaturing action of urea and GuHCl [16]. The unfolding transition of Aes induced by the two chemical denaturants proved to be reversible and more complex than the two-state N ⇆ D transi-

Abbreviations: Aes, acetylesterase from *Escherichia coli*; AFEST, esterase from *Archeoglobus fulgidus*; BFAE, brefeldine esterase from *Bacillus subtilis*; EST2, esterase from *Alicyclobacillus acidocaldarius*; HSL family, hormone sensitive lipase family of the esterase/lipase super-family; CD, circular dichroism; DSC, differential scanning calorimetry; HPLC, high performance liquid chromatography; SDS-PAGE, sodium dodecyl sulfate-polyacrylamide gel electrophoresis; GuHCl, guanidine hydrochloride; TFE, 2,2,2-trifluoroethanol

* Corresponding author. Tel.: +39 081 674255; fax: +39 081 674257.
E-mail address: pompea.delvecchio@unina.it (P. Del Vecchio).

0040-6031/$ – see front matter © 2005 Elsevier B.V. All rights reserved.
doi:10.1016/j.tca.2005.12.006

tion model. This finding was in line with the existence of two structural domains in the model of the native structure of Aes, constructed using the crystal structure of BFAE as a template.

In the present work, by means of differential scanning calorimetry, DSC and circular dichroism, CD, measurements, the stability of Aes, and the single point mutant V20D-Aes against temperature has been investigated. The process is irreversible, but several evidences suggest that the irreversibility is not an intrinsic feature of the conformational transition, being caused by side reactions occurring at high temperature. Thermal denaturation is characterized by a single DSC peak with no shoulders and CD transition curves with a single inflection point. This would suggest a strong coupling between the two structural domains of Aes. Nevertheless the non-coincidence between the denaturation enthalpy change obtained from the area of DSC peak and those calculated by fitting the CD transition curves is an indication that the process cannot be described as a two-state transition.

2. Materials and methods

2.1. Protein purification and sample preparation

Recombinant Aes and a mutated version, V20D-Aes, obtained "by chance" during cloning of the *ybaC* gene, were overexpressed in *E. coli* and purified as previously described [17]. The purity of homogeneous preparations was checked by SDS-PAGE and reversed-phase HPLC. Protein samples were dialyzed against appropriate buffers and concentrated by using an Amicon ultrafiltration apparatus for the following analyses. Aes and V20D-Aes were dissolved in a 20 mM sodium phosphate buffer at pH 7.5 and the concentration determined spectrophotometrically using a theoretical, sequence-based [18], extinction coefficient of 54,500 $M^{-1}\,cm^{-1}$ at 280 nm. Protein solutions for CD and DSC measurements were exhaustively dialyzed by using Spectra Por MW 15,000 membranes against buffer solution at 4 °C. The water used for buffer and sample solutions was doubly distilled. The pH was measured at 25 °C with a Radiometer pHmeter model PHM93.

2.2. Differential scanning calorimetry

DSC measurements were carried out on a Setaram Micro-DSC instrument, interfaced with a data translation A/D board for automatic data acquisition. Data analysis is accomplished with in-house programs [19–21]. A scan rate of 1.0 K min^{-1} was chosen for all experiments. The raw data are converted to an apparent heat capacity by correcting for the instrument calibration curve and the buffer–buffer scanning curve and by dividing each data point by the scan rate and the protein molar concentration in the sample cell. Finally, the excess heat capacity function, $\langle \Delta C_p \rangle$, is obtained by subtraction of the baseline, given by linear extrapolation of the heat capacity of native state [22]. The van't Hoff enthalpy is calculated by the commonly used formula [23]:

$$\Delta_d H_{vH} = 4RT_d{}^2 \langle \Delta C_p(T_d) \rangle / \Delta_d H(T_d) \quad (1)$$

where T_d is the temperature corresponding to the maximum of DSC peak, $\langle \Delta C_p(T_d) \rangle$ is the height of the excess heat capacity at T_d, $\Delta_d H(T_d)$ is the total denaturation enthalpy change calculated by direct integration of the area of the DSC peak and R is the gas constant. The calorimetric to van't Hoff enthalpy ratio is called the cooperative unit CU; the finding that CU is close to one is a necessary condition to state that the denaturation is a two-state transition [23,24].

2.3. Circular dichroism

CD spectra were recorded with a Jasco J-715 spectropolarimeter equipped with a Peltier-type temperature control system (model PTC-348WI). The instrument was calibrated with an aqueous solution of D-10-(+)-camphorsulfonic acid at 290 nm [25]. The molar ellipticity per mean residue, $[\theta]$ ($^\circ\,cm^2\,dmol^{-1}$), was calculated from the equation: $[\theta] = [\theta]_{obs}(mrw)\,(10 \cdot l \cdot C)^{-1}$, where $[\theta]_{obs}$ is the ellipticity (°), mrw is the mean residue molecular weight, 113, C is the protein concentration ($g\,mL^{-1}$) and l is the optical path length of the cell (cm). Cells with 0.2 and 1 cm path lengths and protein concentrations of about 0.1 and 1 mg mL^{-1} were used in the far- and near-UV regions, respectively. CD spectra were recorded with a time constant of 16 s, a 2 nm bandwidth and a scan rate of 5 nm min^{-1}, signal-averaged over at least five scans, and baseline corrected by subtracting a buffer spectrum. Thermal denaturation curves were recorded in the temperature mode at 222 nm and 270 nm, from 25 to 90 °C with a scan rate of 1.0 K min^{-1} and analyzed as already described [6,7,26].

3. Results

The temperature-induced denaturation of Aes and V20D-Aes has been investigated by means of DSC and CD at 20 mM phosphate buffer, pH 7.5. The DSC profiles are shown in Fig. 1, while the far-UV (222 nm) and near-UV (270 nm) transition curves are shown in Fig. 2 for Aes, and Fig. 3 for V20D-Aes. Unfortunately a full thermodynamic characterization of the stability of the two proteins is not possible because the process is irreversible in the investigated conditions; no DSC peak and sigmoidal curve are recorded on the second heating. To try to shed light on this phenomenon several DSC measurements were performed in the following manner: the thermal cycle consists of a first heating stopped near the maximum of the peak; a cooling up to room temperature; and a complete heating up to 85 °C. Interestingly the protein samples subjected to this temperature cycle showed an almost complete reversibility (see Fig. 1). This indicates that the observed irreversibility is due to side reactions occurring at high temperature. Aes possesses nine Cys residues, only six of which appear engaged in disulfide bridges on the basis of the 3D model obtained by using the X-ray structure of BFAE as template [16]. The three free sulfhydryl groups may be involved in side reactions at high temperature, in the unfolded chains, preventing the correct refolding of the polypeptide chain on cooling the solution.

The parameters obtained from the analysis of DSC curves are: (a) for Aes, $T_d = 68$ °C, $\Delta_d H(T_d) = 760$ kJ mol^{-1}

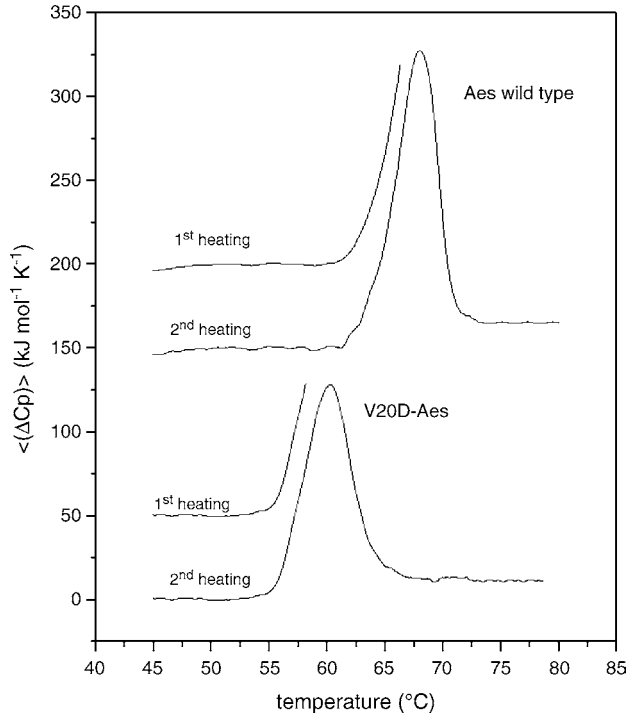

Fig. 1. DSC profiles of Aes and V20D-Aes at pH 7.5, 20 mM phosphate buffer, recorded at a scanning rate of 1 K min^{-1}. Curves are shifted along the *y*-axis for illustrative purposes.

and $\Delta_d C_p = 16\,kJ\,K^{-1}\,mol^{-1}$; (b) for V20D-Aes, $T_d = 61\,°C$, $\Delta_d H(T_d) = 650\,kJ\,mol^{-1}$ and $\Delta_d C_p = 13\,kJ\,K^{-1}\,mol^{-1}$ (see Table 1). The CU values for both proteins are larger than one, indicating that the process is not a two-state transition.

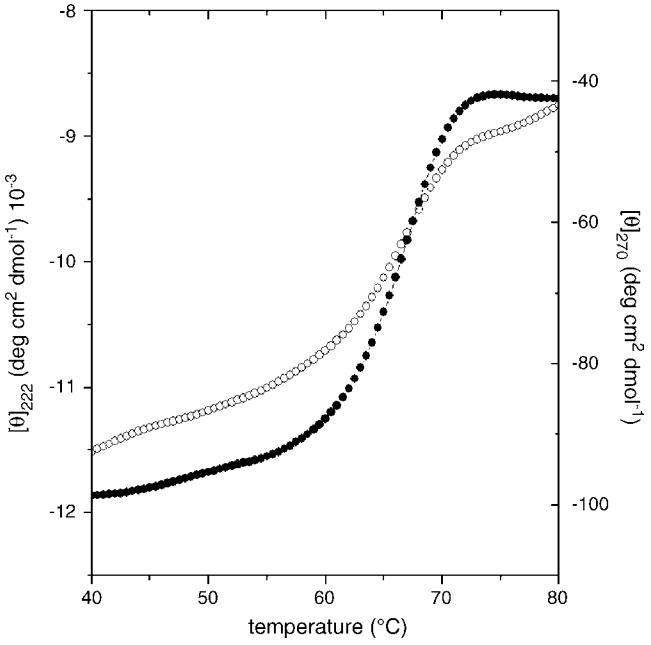

Fig. 2. Temperature-induced transition curves of Aes at pH 7.5, 20 mM phosphate buffer, determined by recording the molar ellipticity at 222 nm (open circles) and 270 nm (filled circles).

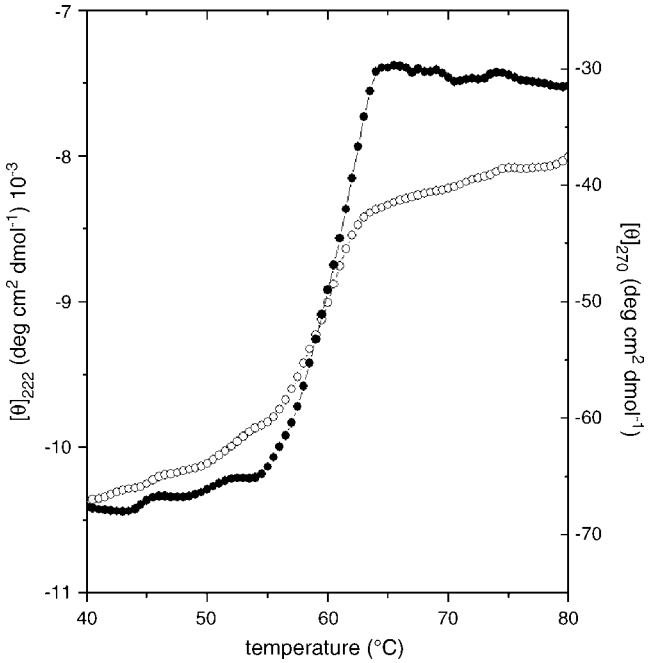

Fig. 3. Temperature-induced transition curves of V20D-Aes at pH 7.5, 20 mM phosphate buffer, determined by recording the molar ellipticity at 222 nm (open circles) and 270 nm (filled circles).

Moreover, even though the process is irreversible, the inflection points of the CD transition curves both in the far-UV and near-UV regions correspond to the T_d values obtained from DSC profiles for both Aes and V20D-Aes. This finding is a further evidence that the irreversibility is not an intrinsic feature of the conformational transition. On this basis we performed an analysis of the CD transition curves by means of the reversible two-state N ⇆ D model. The results are collected in Table 1. It is evident that, while the T_d values are 68 °C for Aes and 61 °C for V20D-Aes regardless of the probe used, the $\Delta_d H(T_d)$ values calculated from CD curves are significantly lower than those obtained from the area of DSC peaks. This indicates that the native structure of Aes does not behave

Table 1
Parameters characterizing the temperature-induced denaturation of Aes and V20D-Aes at pH 7.5, 20 mM phosphate buffer

	Probe	T_d (°C)	$\Delta_d H(T_d)$ (kJ mol^{-1})	$\Delta_d C_P$ (kJ K^{-1} mol^{-1})	CU
Aes	DSC	68	760	16	1.6
	Far-UV CD	68	500	–	–
	Near-UV CD	68	530	–	–
V20D-Aes	DSC	61	630	13	1.6
	Far-UV CD	61	450	–	–
	Near-UV CD	61	490	–	–

Note: CU refers to the cooperative unit given by the calorimetric to van't Hoff enthalpy ratio. Three independent DSC and CD measurements were performed. For CD transition curves the parameter values are calculated by non-linear regression with respect to a N ⇆ D transition model, as described [6,7]. Errors in T_d amount to 0.5 °C, while the uncertainties in the $\Delta_d H(T_d)$ and $\Delta_d C_p$ estimates amount to 5% and 10%, respectively, of the numbers quoted in the table.

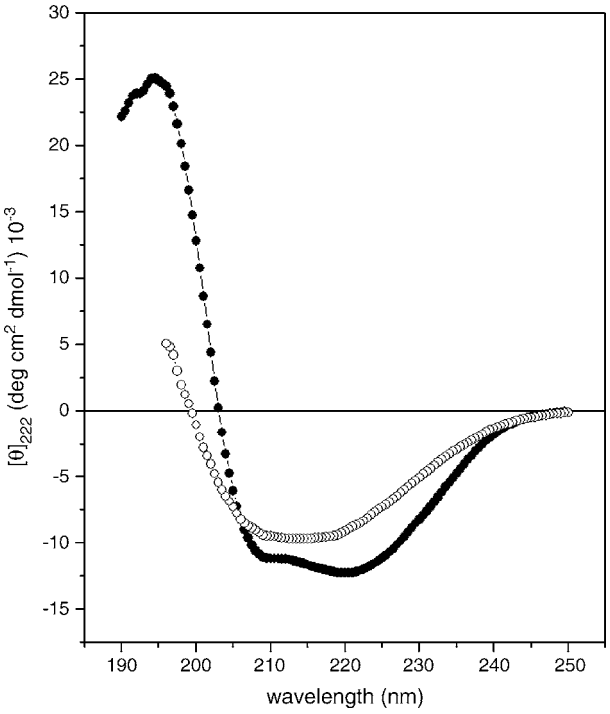

Fig. 4. Far-UV CD spectra of native Aes (filled circles) recorded at pH 7.5 and 20 °C, and thermally denatured Aes (open circles) recorded at 90 °C.

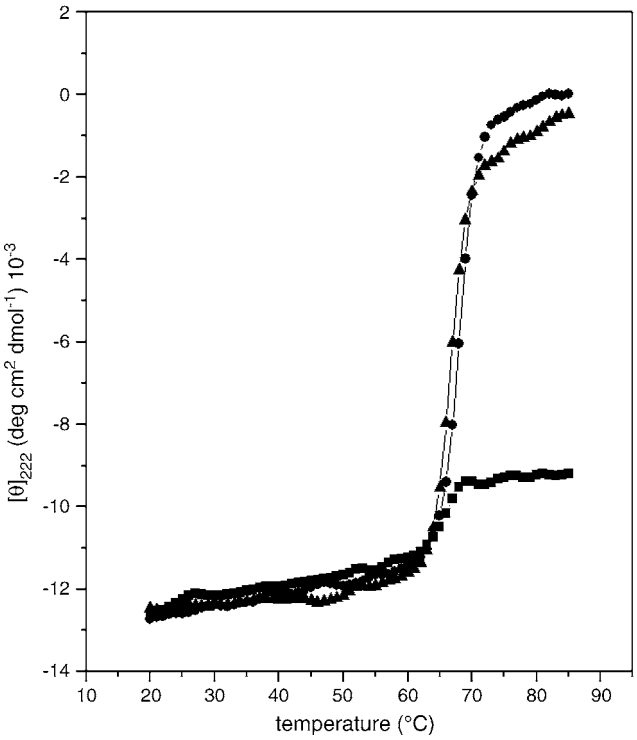

Fig. 5. Temperature-induced transition curves of Aes at pH 7.5 in the absence (squares) and in the presence of 1 M (triangles), and 1.5 M (circles) NaCl, determined by recording the molar ellipticity at 222 nm.

as a single cooperative domain in the temperature-induced denaturation process (this statement holds also for the mutant V20D-Aes).

Another point is the recognition that the denatured state of both Aes and V20D-Aes contains a significant fraction of secondary structure. The far-UV CD spectra of Aes at 20 °C and 90 °C, respectively, at pH 7.5, 20 mM phosphate buffer, are reported in Fig. 4 (similar spectra have been recorded for V20D-Aes; data not shown). Estimation of the secondary structure content, performed by means of DICHROWEB [27,28], provides values in line with those determined from the X-ray structures of thermophilic EST2 [13], and hyperthermophilic AFEST [29], suggesting that Aes can be considered their mesophilic counterpart [16]. On the other hand, the spectrum at 90 °C indicates the presence of significant residual secondary structure in the thermally denatured samples.

In order to clarify this point, thermal transition curves have been recorded in the far-UV region for Aes in the presence of 1.0 M and 1.5 M NaCl, in 20 mM phosphate buffer, pH 7.5 (see Fig. 5). The process is always irreversible, and the denaturation temperature of Aes does not change in the presence of 1.0 M or 1.5 M NaCl: T_d is always 68 °C. However the denatured conformations populated at high temperature under high salt concentrations differ markedly from those populated in the absence of salt, being characterized by a smaller fraction of residual secondary structure elements (i.e., the molar ellipticity at 222 nm is close to zero). These findings suggest that: (a) the conformational features of the thermally denatured state of Aes depend on the properties of the solvent in which it is dissolved; (b) the investigated process is a true conformational transition not really affected by irreversibility; (c) the electrostatic interactions in the denatured state should be responsible of the residual secondary structure [30].

4. Discussion

Experimental data indicate that the temperature-induced denaturation of Aes is not a simple two-state process. The presence of more than a single cooperative domain in the native structure of Aes is supported by the 3D model obtained by using the X-ray structure of BFAE as template and reported in a previous paper [16]. Accordingly, Aes should possess the canonical α/β fold [5] with a central β-sheet constituted by eight strands twisted by about 90°, surrounded by several α-helices. Analysis of the 3D model suggests that the N-terminal part of the chain, approximately the first 50 residues, forms part of a further domain covering the active site of Aes. Such a domain consists of α-helical segments and has already been identified in the X-ray structures of BFAE [14] and AFEST [29]. The existence of two domains in the native structure of Aes allowed the rationalization of the urea- and GuHCl-induced unfolding at 20 °C of both Aes and V20D-Aes [16].

On the other hand, the temperature induced denaturation of both Aes and V20D-Aes is characterized by: (a) a single DSC peak with no shoulders; (b) CD transition curves with a single inflection point in both the far-UV and near-UV regions.

These data indicate a strong coupling of the two structural domains when a physical denaturant such as temperature is used to induce the conformational transition. However, the marked discrepancy existing between the denaturation enthalpy value obtained directly from the area of DSC peaks (760 kJ mol^{-1}) and those calculated by fitting the CD transition curves with respect to the N ⇆ D model (500 kJ mol^{-1}) should be considered a clear indication that the process is not a two-state transition.

Both CD and DSC measurements indicate that V20D-Aes is significantly less stable than Aes; T_d decreases from 68 °C to 61 °C. The decreased thermal stability of V20D-Aes with respect to Aes could be attributed to the desolvating penalty associated with the burial of the charged group from the water contact [31], since the 3D model shows that the Val20 side chain is buried in the native structure of Aes, interacting with the nonpolar side chains of Phe294 and Met301. Otherwise, one could suppose that, to avoid the desolvating penalty, the Asp side chain remains on the protein surface, leaving a cavity in the interior that destabilizes the folded state of V20D-Aes (i.e., the different relative hydrophobicity between Val and Asp plays a role).

Aes can be considered the mesophilic counterpart of the thermophilic EST2 and AFEST, whose conformational stability has already been investigated in our labs [6–9]. The T_d values determined at pH 7.5 in the same experimental conditions are: 68 °C for Aes, 91 °C for EST2 and 99 °C for AFEST. A tentative explanation of the thermal stability difference might be advanced. A large number of sequence and structural factors are thought to be involved in the higher intrinsic thermal stability of thermophilic enzymes. In particular we mention the shortening of surface loops, higher proportion of hydrophobic residues with branched side chains, higher proportion of charged residues at the expense of uncharged polar residues, higher number of salt-bridges and optimisation of electrostatic interactions [32–36]. By combining together the experimental data on the resistance of EST2 and AFEST toward the denaturing action of urea, GuHCl, TFE and temperature with the available structural information, it emerged that the optimisation of charge–charge interactions should be the fundamental factor to enhance the thermal stability of the two esterases [36–39]. Since there is a smaller number of charged residues in Aes with respect to both AFEST and EST2, in agreement with the charged-versus-polar bias identified by Cambillau and Claverie [37], one could surmise that the contribution of charge–charge interactions for the thermal stability of Aes is not so large as in the case of EST2 and AFEST [16]. Work is in progress to clarify the relationship between Aes and the two thermophilic esterases.

Acknowledgments

Work supported by grants from the Italian Ministry for the Instruction, University and Research (M.I.U.R., Rome) and by "Centro Regionale di Competenza per l′Analisi e il Monitoraggio del Rischio Ambientale" (AMRA).

References

[1] G. Manco, E. Adinolfi, F.M. Pisani, V. Carratore, M. Rossi, Biochem. J. 332 (1998) 203–212.
[2] G. Manco, F. Febbraio, E. Adinolfi, M. Rossi, Protein Sci. 8 (1999) 1789–1796.
[3] G. Manco, E. Giosuè, S. D'Auria, P. Herman, G. Carrea, M. Rossi, Arch. Biochem. Biophys. 373 (2000) 182–192.
[4] G. Manco, L. Camardella, F. Febbraio, G. Adamo, V. Carratore, M. Rossi, Protein Eng. 13 (2000) 197–200.
[5] D.L. Ollis, E. Cheah, M. Cygler, B. Dijkstra, F. Frolow, S.M. Franken, et al., Protein Eng. 5 (1992) 197–211.
[6] P. Del Vecchio, G. Graziano, V. Granata, G. Barone, L. Mandrich, G. Manco, M. Rossi, Biochemistry 41 (2002) 1364–1371.
[7] P. Del Vecchio, G. Graziano, V. Granata, G. Barone, L. Mandrich, G. Manco, M. Rossi, Biochem. J. 367 (2002) 857–863.
[8] P. Del Vecchio, G. Graziano, V. Granata, G. Barone, L. Mandrich, M. Rossi, G. Manco, Biophys. Chem. 104 (2003) 407–415.
[9] L. Mandrich, M. Pezzullo, P. Del Vecchio, G. Barone, M. Rossi, G. Manco, J. Mol. Biol. 335 (2004) 357–369.
[10] R. Peist, A. Koch, P. Bolek, S. Sewitz, T. Kolbus, W. Boos, J. Bacteriol. 179 (1997) 7679–7686.
[11] S. Kanaya, T. Koyanagi, E. Kanaya, Biochem. J. 332 (1998) 75–80.
[12] K. Gerber, A. Schiefner, P. Seige, K. Diederichs, W. Boos, W. Welte, Acta Crystallogr. D: Biol. Crystallogr. 60 (2004) 531–533.
[13] G. De Simone, S. Galdiero, G. Manco, D. Lang, M. Rossi, C. Pedone, J. Mol. Biol. 303 (2000) 761–771.
[14] Y. Wei, J.A. Contreras, P. Sheffield, T. Osterlund, U. Derewenda, R.E. Kneusel, U. Matern, C. Holm, Z.S. Derewenda, Nat. Struct. Biol. 6 (1999) 340–345.
[15] N. Sorrentino, G. De Simone, V. Menchise, L. Mandrich, M. Rossi, G. Manco, C. Pedone, Acta Crystallogr. D: Biol. Crystallogr. 59 (2003) 1846–1848.
[16] P. Del Vecchio, G. Graziano, V. Granata, T. Farias, G. Barone, L. Mandrich, G. Manco, M. Rossi, Biochemistry 43 (2004) 14637–14643.
[17] L. Mandrich, E. Caputo, B.M. Martin, M. Rossi, G. Manco, J. Biol. Chem. 277 (2002) 48241–48247.
[18] S.C. Gill, P.H. von Hippel, Anal. Biochem. 182 (1989) 319–326.
[19] G. Barone, P. Del Vecchio, D. Fessas, C. Giancola, G. Graziano, J. Thermal Anal. 38 (1992) 2779–2790.
[20] F. Catanzano, C. Giancola, G. Graziano, G. Barone, Biochemistry 35 (1996) 13378–13385.
[21] G. Graziano, F. Catanzano, C. Giancola, G. Barone, Biochemistry 35 (1996) 13386–13392.
[22] E. Freire, R.L. Biltonen, Biopolymers 17 (1978) 463–479.
[23] P.L. Privalov, Adv. Protein Chem. 33 (1979) 167–241.
[24] Y. Zhou, C.K. Hall, M. Karplus, Protein Sci. 8 (1999) 1064–1074.
[25] S.Y. Venyaminov, J.T. Yang, in: G.D. Fasman (Ed.), Circular Dichroism and the Conformational Analysis of Biomolecules, Plenum Press, New York, 1996, pp. 69–107.
[26] E. Shehi, V. Granata, P. Del Vecchio, G. Barone, P. Fusi, P. Tortora, G. Graziano, Biochemistry 42 (2003) 8362–8368.
[27] A. Lobley, L. Whitmore, B.A. Wallace, Bioinformatics 18 (2002) 211–212.
[28] W.C. Johnson, Methods Biochem. Anal. 31 (1985) 61–163.
[29] G. De Simone, V. Menchise, G. Manco, L. Mandrich, L. Sorrentino, D. Lang, M. Rossi, C. Pedone, J. Mol. Biol. 314 (2001) 507–518.
[30] C.N. Pace, R.W. Alston, K.L. Show, Protein Sci. 9 (2000) 1395–1398.
[31] L. Xiao, B. Honig, J. Mol. Biol. 289 (1999) 1435–1444.
[32] A.M. Lesk, Biophys. Chem. 105 (2003) 179–182.
[33] M.M. Gromiha, M. Oobatake, A. Sarai, Biophys. Chem. 82 (1999) 51–67.

[34] C. Vieille, G.J. Zeikus, Microbiol. Mol. Biol. Rev. 65 (2001) 1–43.
[35] R. Jaenicke, G. Bohm, Methods Enzymol. 334 (2001) 438–469.
[36] J.M. Sanchez-Ruiz, G.I. Makhatadze, Trends Biotechnol. 19 (2001) 132–135.
[37] C. Cambillau, J.M. Claverie, J. Biol. Chem. 275 (2000) 32383–32386.
[38] K. Suhre, J.M. Claverie, J. Biol. Chem. 278 (2003) 17198–17202.
[39] V. Granata, P. Del Vecchio, G. Barone, E. Shehi, P. Fusi, P. Tortora, G. Graziano, Int. J. Biol. Macromol. 34 (2004) 195–201.